Capturing a light pulse in a short high-finesse cavity

B. P. J. Bret,* T. L. Sonnemans,† and T. W. Hijmans‡
Van der Waals–Zeeman Instituut, Valckenierstraat 65, 1018 XE Amsterdam, The Netherlands
(Received 7 August 2002; published 20 August 2003)

We describe a method to couple a light pulse into a cavity with arbitrarily high finesse, with an efficiency that in theory can approach 100% even if the pulse duration is much longer than the round-trip time of the cavity. The spectrum of the pulse is compressed into a single narrow mode in an adiabatic and reversible way. The method uses an input coupler with a variable effective reflectivity which is adapted to match the known temporal shape of the pulse. In addition to a theoretical description of the method, we demonstrate the principle experimentally.

DOI: 10.1103/PhysRevA.68.023807 PACS number(s): 42.60.Da, 07.60.Ly, 42.79.Nv

I. INTRODUCTION

There exist many examples of applications in optics where a combination of high (peak) intensity and narrow spectral width is desirable or even essential. Examples are high-resolution uv and vuv (vacuum ultraviolet) spectroscopy [1,2] where second-harmonic generation or four-wave mixing is needed to produce the appropriate wavelengths or laser isotope separation [2–4], where the yield depends on intensity but resolution is essential due to the smallness of isotope shifts. Generally speaking, high power and high resolution are mutually exclusive; the first belongs to the realm of pulsed lasers and the second to that of cw light sources. This paper describes a way in which this dichotomy can be circumvented: we aim to obtain a light power characteristic of pulsed sources yet at cw bandwidths. We describe the theoretical principle of the method and present experimental corroboration of the idea.

It is simple to capture a pulse in a cavity if its duration τ_{p} is less than the round-trip time τ_{cav}. One can simply use a variable input coupler, similar to, for example, *Q*-switched lasers or regenerative amplifiers [5], to 'slam the door shut' so to say, after the pulse has entered. In this case the full pulse energy is coupled into the cavity, but the bandwidth is not reduced. To achieve the desired spectral narrowing we need the opposite situation where τ_{cav} is much smaller than τ_{p}. In the frequency domain this corresponds to the situation where only one cavity mode overlaps with the pulse spectrum, in other words, the free-spectral range W_{FSR} of the cavity is larger than the pulse bandwidth *W*. Clearly, if we now try to admit the pulse into the cavity, it will start leaking out again well before the entire pulse has passed the input coupler, much like filling a ''leaky bucket.'' Alternatively if we ''close the door'' too early, only a small part of the pulse energy is captured. Consequently either we lose power or compromise on obtainable bandwidth or both.

The method described here is based on the following idea: rather than using the variable input coupler as an open/close switch, we slowly change the reflectance of the input coupler from 0 to 1 on a time scale comparable to τ_p, hence much longer than τ_{cav}. There exists an appropriate choice of switching function of the reflectance which leads to zero loss: we choose the value of the input reflectance at each instant in time such that the fraction of the light already in the cavity that is transmitted back out exactly cancels the reflected fraction of the input pulse. We can call this dynamic impedance matching.

Unlike the usual situation where a cavity acts as a filter [6], discarding the frequency components outside its resonant modes, we end up here with all the pulse energy inside the cavity circulating at one of its resonance frequencies. The spectrum of the pulse has been squeezed into the single-cavity mode. We will show that this is possible, provided we know the shape and arrival time of the input pulse as well as its central frequency. If implemented successfully the result of the scheme is remarkable: we have transformed a pulse of light into a nearly continuous-wave signal which decays on a time scale only limited by the finesse *F* of the cavity, which can result in a spectral width much less than that of the original pulse if *F* is high enough.

The fact that the full energy is transferred in the cavity actually leads to an increase in power in the cavity relative to that of the incoming pulse, contrary to what one might guess. The reason is simply energy conservation: the peak power inside the cavity is just the pulse energy divided by the cavity round-trip time τ_{cav}, which by assumption is much smaller than the pulse duration τ_p.

An essential element in the practical implementation of the scheme is the variable input coupler for which we use a polarizing beam splitter combined with a Pockels cell and polarization optics, and precisely timed switching electronics.

Experimentally our motivation for developing the method is efficient intracavity second harmonic generation [7]. However a very different use of the scheme can be envisaged: reversible storage and subsequent release of a light pulse with almost 100% efficiency. As the method is essentially adiabatic, the stored light can readily be released again by reversing the process. The holding time is limited only by the finesse of the closed cavity. This application bears some analogy with experiments that have attracted considerable

*Present address: Universiteit Twente, Postbus 217, 7500AE Enschede, The Netherlands.
†Present address: Joh. Enschedé, Postbus 464, 2000 AL Haarlem, The Netherlands.
‡Electronic address: hijmans@science.uva.nl

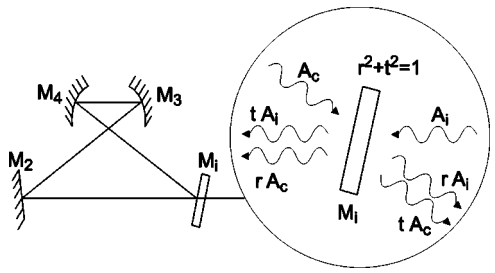

FIG. 1. Simplified drawing of a ring cavity with three high reflectivity mirrors M_2 through M_4, and a mirror M_i with dynamic reflectivity $R(t)$, used as input coupler. In the inset are shown four waves, two inside and two outside the cavity, traveling towards and away from M_i. The wave leaving the cavity can be made to vanish by destructive interference for an appropriate value of $R \equiv r^2$.

attention recently. In papers from two different groups [8,9] it was shown that light could be effectively ''slowed down'' to zero velocity and stored in a medium of atomic vapor. These experiments use a control field to transform the character of a coupled light-atom coherence from almost purely lightlike to almost atomic, in a reversible adiabatic manner. Our capturing of pulses in a cavity proceeds along somewhat analogous lines. The ''atomiclike'' state of Refs. [8,9] can be compared to our cavity with the light trapped inside. Clearly the analogy is far from complete as our experiment is purely classical. One important practical consequence of this difference is that, unlike the atom, the narrow-band light inside the cavity is actually available for intracavity experiments. We should state that to perform such capture and release experiments an improved version of our experiment, which at present is in a proof of principle stage, is required and we will not pursue this issue experimentally in this paper.

We will first outline the theory in Sec. II. In Secs. III and IV we discuss the experimental methods, in Sec. V we present the experimental results, and we conclude with Sec. VI.

II. THEORETICAL DESCRIPTION OF THE METHOD

In this section we analyze the theory of the method using a time-domain picture. This turns out to be more natural and transparent than using the frequency domain, primarily because the switching done with the variable input coupler is adapted to the temporal shape of the light pulse. However, when we consider experiments, the main goal of the method is to provide a spectral narrowing of the captured light and measurement of this narrowing is best performed as directly as possible, hence in the frequency domain.

In Fig. 1 we show a schematic representation of a ring cavity. The input coupling mirror M_i has a variable coefficient of reflectivity and mirrors M_2–M_4 are considered perfectly reflecting. To simplify the discussion we will assume in this analysis that the pulses are Fourier-transform limited. In the actual experiment described below this assumption is not strictly true. Yet, the experiments described below will empirically show that this method is still applicable to the case where the bandwidth of the impinging pulse significantly exceeds the Fourier transform limit. The inset of Fig. 1 shows a snapshot in time at an instant when some light is already circulating in the cavity and some light is impinging on M_i. We now consider four complex field amplitudes: the amplitude A_i of light impinging on M_i, the reflected light $A_r \equiv rA_i$, where $|r|^2 \equiv R$ is defined as the reflectivity coefficient, the amplitude A_c circulating inside the cavity measured directly before returning to M_i, and the amplitude $A_t = \sqrt{1-r^2}A_c$ transmitted from the cavity to the outside through M_i. The amplitudes we compare actually refer to the values on the axis of a Gaussian mode. As all amplitudes are compared at the same plane in the cavity, all have the same waist.

If the cavity is exactly on resonance we have as usual that the phase of A_t is exactly opposite to that of A_r [6]. The following condition now holds if we require that the total reflected intensity be zero:

$$A_i r = -A_c \sqrt{1-r^2}. \tag{1}$$

For Fourier-transform limited pulses, this condition can be realized at all times if the cavity is resonant at the central frequency component of the pulse. In this case this input coupler acts as a perfect one-way light valve.

A realistic cavity will have a finite ring down time τ_r due to losses such as absorption or nonperfect mirrors. By considering the rate of change of the total energy outside and inside the cavity when all the light is coupled in, we find a relation between A_c and A_i:

$$\frac{\partial A_c^2(t)}{\partial t} = \frac{A_i^2(t)}{\tau_{\mathrm{cav}}} - \frac{A_c^2}{\tau_r}. \tag{2}$$

Let us first consider an ideal cavity without losses so that τ_r^{-1} vanishes. Then using Eq. (1) the effective reflectivity of the input coupler is written as

$$R \equiv r^2 = \frac{A_c^2}{A_c^2 + A_i^2}. \tag{3}$$

Using Eq. (2) we eliminate A_c through

$$\tau_{\mathrm{cav}} A_c^2(t) = \int_{-\infty}^{t} d\tau A_i^2(\tau). \tag{4}$$

Hence, for a given input pulse shape we can directly calculate the reflectivity function $R(t)$ appropriate for coupling all the energy into the cavity. In Fig. 2 we give an example for a Gaussian pulse of unit width and height and $\tau_{\mathrm{cav}} = 0.086$. This ratio of τ_{p} and τ_{cav} corresponds roughly to the experimental value to be investigated later. We see that for this lossless case, at large positive times the cavity is completely closed and the light circulates forever at a single, infinitely narrow, frequency band around the cavity resonance frequency with an intensity that exceeds that of the peak of the input pulse by more than an order of magnitude. In fact the effect of switching the input coupler is to adiabatically change the spectrum from the initial Fourier transform of the pulse shape into that corresponding to the Lorentzian cavity spectrum; the frequency components of the pulse are gradu-

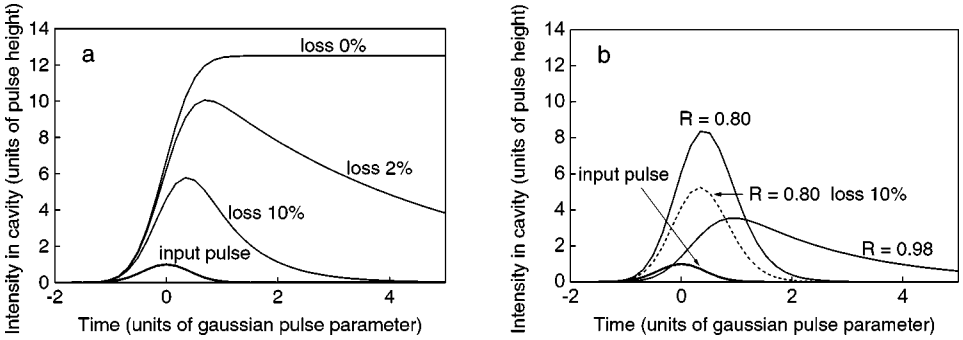

FIG. 2. Intensity inside the cavity as a function of time for a Gaussian input pulse of unit full width at half maximum (FWHM) and $\tau_{\mathrm{cav}}=0.086$. In (a) curves are compared for the optimally switched reflectivity, in a cavity with various losses. In (b) we show curves for the same cavity but with fixed reflectivity of M_i for $R=0.80$ and $R=0.98$. The solid lines correspond to 2% loss. The dashed line corresponds to 10% loss and $R=0.80$.

ally pushed closer to the central cavity mode as the cavity finesse increases. What is clear is that this process is very different from filtering: we are not simply projecting out the cavity mode out of the offered frequency spectrum.

The use of Gaussian pulses is not essential. In principle the method works even for a square-wave pulse if its duration exceeds τ_{cav}. In this case the time-dependent reflectivity $R(t)$ changes in small discrete steps every time the leading edge of the pulse inside the cavity arrives back at the input coupler. Although unpractical to implement, the peak electric field inside the cavity after capture is larger than the electric-field intensity of the incoming pulse by exactly the factor $\tau_{\mathrm{p}}/\tau_{\mathrm{cav}}$.

We defer to Sec. IV a discussion of how in practice we match the cavity length to the central frequency of the pulse. In Sec. III we will comment on the possibility to allow for a modest chirp rather than using purely transform limited pulses.

We now relax the requirement that the losses are zero. Even with very good components a realistic minimum power loss is 2% per round trip. Thus $\tau_r \approx 50\tau_{\mathrm{cav}}$. We can solve Eqs. (1) and (2) including finite losses. The results for both 2% and 10% losses are shown in Fig. 2(a). For the same $R(t)$ but different losses the stored intensity now decays on a time scale characteristic of the additional loss.

In Fig. 2(b) we show the intracavity intensity versus time for fixed reflectivity for comparison. Two cases are shown: $R=0.80$, which corresponds to the highest possible peak intensity, and $R=0.98$. The latter curve decays nearly as slowly as in the switched case but the peak amplitude is much smaller. For higher loss rates the advantage of the time dependent R diminishes. For 10% loss the slower decaying tail is still just visible. This loss rate marks the boundary of the usefulness of the method and corresponds to a ring down time of the order of the pulse duration.

One may well ask how critically the exact temporal behavior of $R(t)$ determines the fraction of light that can be coupled into the cavity. To check this we relaxed the condition, Eq. (1), and replaced the optimal switching function $R(t)$ by one that results from an exponentially decreasing voltage on the Pockels cell used to implement the switching mirror, as described in the following section. Such an exponentially decreasing voltage leads to the following dependence of the effective reflectivity:

$$R(t)=\frac{1}{1+\tan^2\theta}, \tag{5}$$

where $\theta=(\pi/2)(1-\Theta(t)[1-\exp(-t/\tau_{\mathrm{s}})])$ with τ_{s} the relaxation time of the Pockels cell and switching electronics and $\Theta(t)$ the unit step function. We will describe this switch in detail below in Sec. IV. As can be seen from Fig. 3, $R(t)$ differs significantly from the ideal case but surprisingly the total power coupled into the cavity is hardly affected. Curve c in Fig. 3 is delayed relative to curve b by 0.5 in these units. Even though this timing error is several times τ_{cav} the resulting loss in coupling efficiency is rather modest. This robustness is a very useful feature for experimental implementation.

A comparison of Figs. 2 and 3 indicates that for any fixed reflectivity of the input coupler the signal decays faster than for the switched case for given losses. As stated before this implies that in the frequency domain the spectrum in the switched case is always narrower. Using standard methods

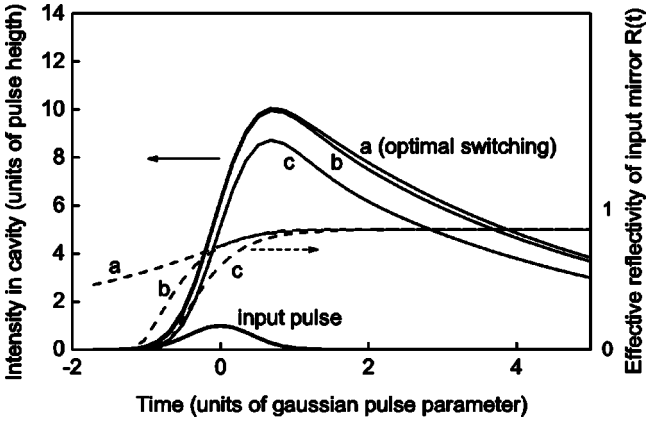

FIG. 3. Intensity in the cavity as a function of time for the same parameters as in Fig. 2. We compare the case of the optimal switching function $R(t)$ (dashed curve *a*) and a form of $R(t)$ that is experimentally easy to implement (dashed curves *b* and *c*). The corresponding resulting intensity is shown as full lines labeled *a*, *b*, and *c*. All curves are for 2% loss.

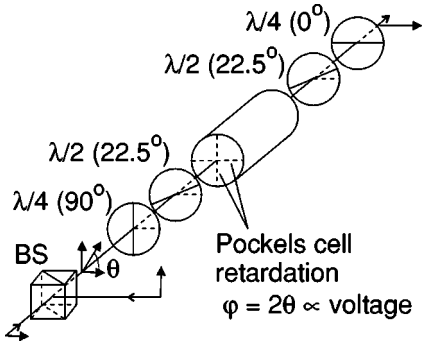

FIG. 4. The input coupler consists of a polarizing beam splitter BS, a Pockels cell, two half-wave plates $\lambda/2$, and two quarter-wave plates $\lambda/4$. The lines on the wave plates indicate the orientations of the optical axes. The full arrows indicate the direction of polarization. The voltage on the Pockels cell is chosen so as to always give horizontally polarized output.

[6] we can find the expression for the width of the frequency spectrum for fixed reflectivity, for the case of a Lorentzian spectrum of the incident light, which we give for later reference:

$$W_{\mathrm{FWHM}}=\frac{1}{\sqrt{2}}[-w^2-W^2+\sqrt{(w^2+W^2)^2+4w^2W^2}]^{1/2}. \tag{6}$$

Here W is the bandwidth of the incident light and the width of one cavity mode $w\equiv W_{\mathrm{FSR}}/F$ for a ring cavity is given by

$$w=W_{\mathrm{FSR}}\frac{2}{\pi}\arcsin\left(\frac{1-\sqrt{RR_L}}{2(RR_L)^{1/4}}\right). \tag{7}$$

Here R_L determines the losses, it should be interpreted as the reflectivity of a mirror mounted instead of one of the perfect mirrors in a lossless but otherwise identical cavity.

III. THE VARIABLE INPUT COUPLER

In the preceding section we assumed that one of the mirrors of the cavity has a variable reflectivity. In reality we use four highly reflecting mirrors ($R\approx 0.9985$) and the light is coupled into the cavity using the device depicted in Fig. 4. The input coupler consists of a polarizing beam splitter, a Pockels cell (Linos CPC8IM), two half-wave plates, and two quarter-wave plates. In fact, the quarter-wave plates are not essential and they are absent in the experiment, but we add them here for clarifying reasons. The principle of the device is as follows: the light circulating in the cavity is horizontally polarized. The light that is coupled into the cavity has a vertical polarization. Consequently, just after the polarizing beam splitter the polarization makes an angle with the horizontal plane that depends on the ratio of the amplitude of the light that has just entered the cavity and that which has made at least one round trip. The combination of Pockels cell and retardation plates acts as a rotator for linear polarization. If at each time the voltage on the Pockels cell is adjusted to a value which ensures that this rotation turns the polarization into the horizontal plane, we are in the situation where all the light is coupled into one cavity mode with horizontal polarization, no light is coupled back out. At the end when no more light impinges on the beam splitter, the voltage on the Pockels cell is zero, the polarization is not rotated anymore, and the cavity is therefore closed.

There is a simple correspondence between the rotation angle $\theta(t)$ and the reflectivity $R(t)$ introduced before; it is given by Eq. (5) above.

To see that the combination of retardation plates and Pockels cell acts as a polarization rotator we write the polarization as a two-component vector (η,ξ). The components η and ξ of this vector are the normalized amplitudes with horizontal and vertical polarization, respectively. In this basis a half-wave plate oriented such that its optical axis makes an angle of 22.5^{o} with the horizontal, has the following matrix representation:

$$\mathbf{H}=\frac{1}{\sqrt{2}}\begin{pmatrix}1 & 1\\ 1 & -1\end{pmatrix}. \tag{8}$$

We further introduce a symmetric phase-shift operator:

$$\mathbf{P}(\varphi)=\begin{pmatrix}\exp(i\varphi/2) & 0\\ 0 & \exp(-i\varphi/2)\end{pmatrix}. \tag{9}$$

Equations (8) and (9) are the usual Jones matrices [10]. The Pockels cell is a variable retarder with retardation angle proportional to the applied voltage. It is now easily verified that the assembly depicted in Fig. 4 is indeed a pure polarization rotator:

$$\begin{pmatrix}\cos\theta & \sin\theta\\ -\sin\theta & \cos\theta\end{pmatrix}=\mathbf{P}(-\pi/2)\cdot\mathbf{H}\cdot\mathbf{P}(2\theta)\cdot\mathbf{H}\cdot\mathbf{P}(\pi/2), \tag{10}$$

where $\mathbf{P}(\pm\pi/2)$ are due to the quarter-wave plates and the rotation angle of polarization θ is half the retardation angle of the Pockels cell.

We always choose the rotation angle such that the output polarization is horizontal; the device rotates over an angle equal in size but opposite to that of the linear input polarization relative to the horizontal direction. Because the optical axis of the two quarter-wave plates is in the horizontal plane, we can simply omit the quarter-wave plate on the output side. The quarter-wave plate at the input side can also be omitted. This introduces a constant phase shift of $\pi/2$ between the two polarization components. The output polarization is still linear but at the input side the polarization is now elliptical. One can show that the system self-adjusts to this constant over-all phase change if the cavity is kept at resonance and operates in essentially the same way.

Pulsed dye amplifiers, such as the one used in our experiments, rarely put out Fourier-transform limited pulses. Often a small amount of chirp is present. If this chirp is known and reproducible, it can in principle be compensated for. This could be done by changing the cavity length while the pulse enters, using a piezodriven mirror or by a second Pockels cell used without the half-wave plates. Alternatively, one can

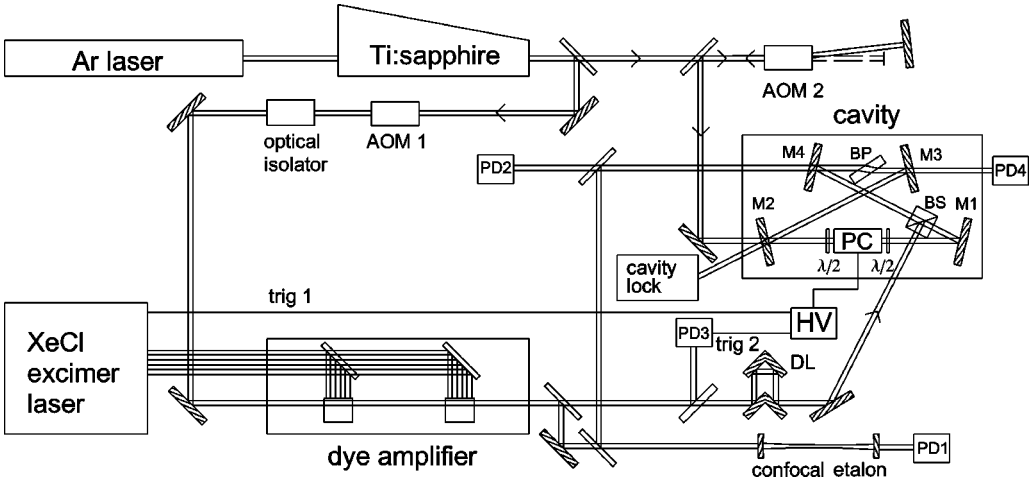

FIG. 5. Drawing of the experimental setup. The simplified cavity of Fig. 1 has been modified by replacing the input coupler M_i by a mirror M_1 and by adding the Pockels cell–based input coupler instead. The polarizing beam splitter is denoted BS, the Pockels cell PC, the two half-wave plates $\lambda/2$, and the Brewster plate BP. PD1 through PD4 are photodiodes for diagnostics and control. PD2 and PD4 monitor the signal and reference intensity inside the cavity, respectively. The confocal etalon is used for recording the frequency spectrum. The frequencies of signal and reference beams are shifted by about 150 MHz each by two acousto-optical modulators AOM1 and AOM2. Adjustment of timing for the electronic switch is made with a 7-m-optical delay line DL and an adjustable length of cable marked TRIG 2. We have omitted in this figure the lenses and telescopes needed for the mode matching of the signal and reference beams to the cavity.

argue that a partial compensation of the chirp can be obtained without any additional elements by choosing the angle of the optical axes of the two half-wave plates in Fig. 4 slightly different from 22.5^o. If this angle was 0^o the Pockels cell would act as a pure retarder. It is thus intuitively reasonable that at angles different from 22.5^o when a pure polarization rotation takes place, the device combines the effects of rotation and retardation. The chirp compensation can have both signs, but is not necessarily linear and depends on the precise form of the time dependence of θ defined below Eq. (5). The analysis of this case is rather involved and the experiments are inconclusive. Hence we do not pursue this point further.

IV. EXPERIMENTAL METHODS

In this section we describe the experimental setup and methods. In Fig. 5 we show the experimental apparatus. The cavity itself has a length of 0.65 m corresponding to $\tau_{\mathrm{cav}} = 2.2$ ns and $W_{\mathrm{FSR}} = 460$ MHz. A cw beam, of 600 mW at a wavelength of 730 nm, from a Ti:sapphire laser (Coherent 899) is split in two parts, one of which, the signal beam, is amplified in a single-stage pulsed dye amplifier (Lambda Physik FL 2003) pumped by an excimer laser (Lambda Physik LPX210i) while the other, the reference beam, serves to lock the cavity. The signal beam provides a pulse of 25 ns duration and a characteristic energy of several tens of μJ to be captured in the cavity. Both signal and reference beams are shifted ≈ 150 MHz in frequency using acousto-optic modulators (AOM's). For the reference beam a double-pass AOM (AOM2 in Fig. 5) is used which allows the frequency to be varied over about 30 MHz, without changing the direction of the beam. This allows for compensation of small frequency shifts introduced by the dye amplifier in the signal arm.

One of the cavity mirrors is mounted on a piezo which is used to vary the cavity length in order to lock the cavity to a resonance for the reference beam. To allow the reference beam into the cavity mirror M_2 has a transmission coefficient of 0.5%. The variable input coupler described in the preceding section is embedded inside the cavity. The Pockels cell is normally switched off and hence the input coupling device is transparent apart from small absorption and reflection losses. The combined losses of the cavity mirrors and the intracavity elements limit the finesse of the cavity to about 60. This corresponds to roughly 10% losses or a ring down time $\tau_r \approx 10\tau_{\mathrm{cav}}$. These comparatively high losses are primarily due to not quite optimal components, particularly the Pockels cell, polarizing beam splitter, and wave plates.

The pulse from the dye amplifier is introduced into the cavity using the following procedure: we switch the voltage on the Pockels cell from 0 to 4 kV about 1 μs before the firing of the excimer laser. The 4 kV voltage corresponds to a retardation of approximately π corresponding to a $\pi/2$ polarization rotation as explained in the preceding section. After the amplified pulse is produced a small part of it is picked off and led to a fast photodiode (PD3) to serve as a trigger for a fast high-voltage switch. This switch, which we describe in detail below, brings back the voltage on the Pockels cell from 4 to 0 kV in a precisely timed fashion in ≈ 10 ns, about half of the pulse duration. The timing of this trigger signal relative to the actual arrival time of the pulse at the polarizing beam splitter in the cavity is determined using a variable cable length combined with an optical delay line of about 7 m.

The reference beam traverses the cavity in the opposite direction as the pulsed signal light. With the Pockels cell switched off the cavity is locked to a resonance for the reference beam using the Hänsch Couillaud method [11]. Since the phase of the cavity mode is set by the input beam in such

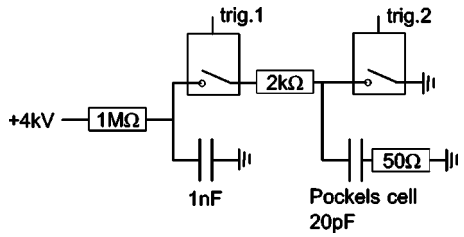

FIG. 6. High-voltage switching electronics for the Pockels cell. The triggers TRIG. 1 and TRIG. 2 are TTL level signals for on and off switching. TRIG. 1 also triggers the excimer laser and TRIG. 2 is taken directly from the fast photodiode PD3 measuring the amplified pulse.

a way that after one round trip the cavity mode and the input beam interfere constructively, any necessary stationary phase difference between the two beams is automatically taken care of. The astigmatism of the cavity resulting from the two curved mirrors is compensated [12] by a 1-cm-thick BK7 brewster plate. This plate can be replaced by a frequency doubling crystal of similar length and refractive index.

The time constant of the locking scheme is of the order of 10^{-4} s, which is slow enough to ensure that the cavity stays in lock when the Pockels cell is briefly switched on and off for about 1 μs to admit the pulse. The pulsed amplification scheme introduces a frequency shift of typically 20 MHz in the output of the signal beam. This shift varies and increases gradually with aging dye. To ensure that the center frequency of the signal coincides with the reference frequency we compare the spectrum of both beams using a confocal etalon with $W_{\mathrm{FSR}}=150$ MHz, and compensate for the difference using the double-pass AOM. The length of the confocal etalon is fixed and to measure the spectrum we slowly scan the frequency of the Ti:sapphire laser. The amplified pulses are sent through the etalon simultaneously with the reference beam. The pulsed light is detected using ''sample and hold'' electronics synchronized with the firing of the excimer laser. The scan time over one FSR of the etalon is about 10 s. This ensures sufficient resolution when firing the excimer laser at 10 Hz or higher.

The confocal etalon serves a second purpose, we use it to measure the spectrum of the light that is stored in the cavity. For this we use the leakage through one of the high reflecting cavity mirrors: M_4 in Fig. 5. Only about 10^{-4} of the light present in the cavity leaks out this way but this is sufficient to send through the etalon and perform a frequency measurement. Again we scan the frequency of the Ti:Sapphire laser, affecting both reference and signal beams in the same way. The cavity lock follows the scanning reference beam frequency and hence the cavity also stays in resonance for the amplified pulsed signal. The signal pulses are captured in the cavity and the spectrum of the leakage light through M_4 is determined.

A final note on the experimental setup concerns the implementation of the switching of the Pockels cell, illustrated in Fig. 6. The switching is done with two fast solid-state high-voltage switches. Both switches act as effective short circuit upon a transistor-transistor logic (TTL) trigger. The first one (Behlke HTS50-06) switches the voltage across the Pockels cell from 0 to 4 kV. This switch is triggered simultaneously with the excimer laser. The actual firing of the excimer laser is delayed with respect to this trigger by about 1.3 μs with a pulse-to-pulse fluctuation of 0.2 μs. When the laser has fired, the optical signal is used to trigger a second fast switch (Alphalas HVS 4000-F) which short circuits the Pockels cell. This second switch has an almost instantaneous (within a few ns) and practically jitter-free response. We found that the second switch, being driven by a TTL level trigger, is rather sensitive to high-voltage cross talk from the first switch which initially caused it to operate at unwanted moments. This problem was solved by empirically adding resistors and parallel capacitors. These also served to set time constant with which the voltage across the Pockels cell drops to the desired value of 10 ns, about half the pulse duration. The additional circuit elements have been omitted in Fig. 6 for simplicity. As mentioned earlier, the timing of the second switch is fine tuned with the optical and electrical delay lines. The resulting voltage on the Pockels cell is an exponential decrease from 4 to 0 kV with a time constant τ_s of typically 10 ns. The resulting effective reflectivity is obtained using Eq. (5). It looks qualitatively like the dashed curve *b* in Fig. 3.

V. EXPERIMENTAL RESULTS

To experimentally corroborate the ideas outlined in the first two sections we perform two types of experiments; in the time domain and in the frequency domain. The light present inside the cavity can be monitored as a function of time by observing the leakage light through M_4 on a fast photodiode. Alternatively, we can obtain the power spectrum of this leakage light by guiding it through the confocal etalon, integrating the pulse, and detecting its magnitude as a function of the laser frequency.

The procedure followed to optimize the energy that can be stored in the cavity is to empirically vary the relative frequency of the reference and signal beams and the timing of triggering of the second high voltage switch in Fig. 6, until the power is maximized and the bandwidth minimized. Introducing a deviation from 22.5^{o} of the angle of the half-wave plates relative to the horizontal polarization direction to compensate for a possible chirp had little effect, and consequently all measurements were taken at the normal orientation of these wave plates. Once the optimal setting was found the situation was stable and the pulse-to-pulse reproducibility proved sufficient to ensure a reliable operation.

In Figs. 7(a) and 7(b) we show the intensity of light leaking through M_4 in the time and frequency domain, respectively. We compare the pulse stored in the switched cavity with the pulse as it is admitted. The latter is measured with an open input coupler (Pockels cell at constant $V=4$ kV) and the cavity blocked so that the light cannot complete the first round trip. This signal has exactly the temporal profile of the pulse from the amplifier, although it is in fact smaller because the polarizing cube rejects a part of the incoming beam. If we take the leakage light from the blocked cavity as an effective definition of our input pulse, we eliminate the effect of rejection by the polarizing cube and we can directly

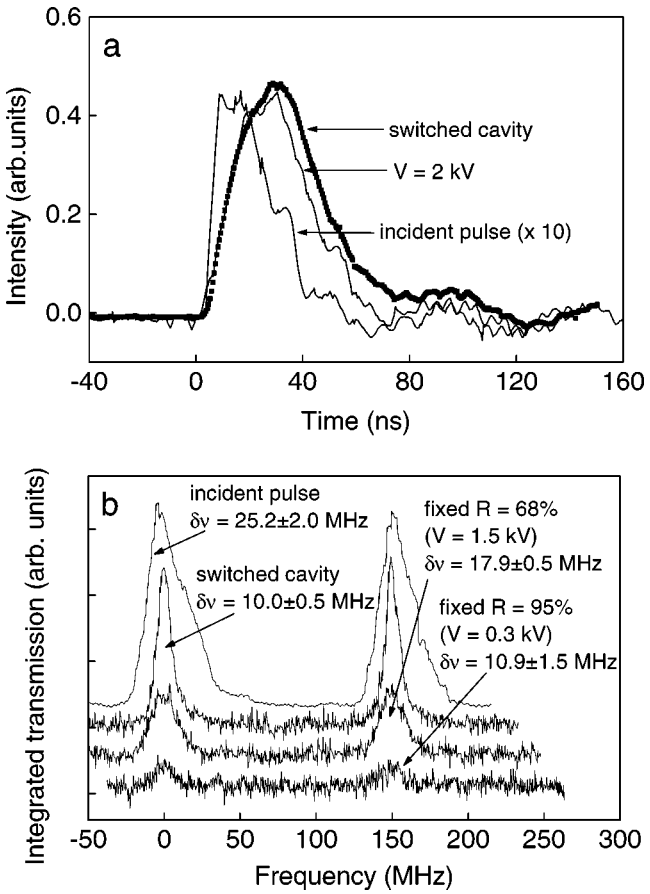

FIG. 7. In (a) we show the stored pulsed light in the cavity vs time, measured using the leakage through M_4 on PD_2. This is compared with the time trace obtained from the incoming pulse in a blocked cavity (see text) and a trace for a fixed cavity with $V=2$ kV. In the bottom panel (b) we compare the power spectrum of the input pulse with that obtained for a switched cavity and a cavity with two different effective reflectivities of the input coupler. The spectrum is proportional to the integrated intensity transmitted through the confocal etalon. The scale of the lower three spectra can be directly compared. The reference spectrum is measured before the cavity, therefore its scale cannot be compared. The zero of the frequenccy scale is set arbitrarily at the position of the left transmission peak.

determine the amplifying effect of the cavity. As can be seen the signal becomes approximately a factor of 10 larger if the cavity is opened and the input coupler switched appropriately, optimized for maximum signal. In Fig. 7 we also show the signal leaking from a cavity with a fixed Pockels cell voltage of 2 kV. For fixed input coupling this choice of voltage couples the maximum energy into the cavity. From Fig. 7(a) we find that the pulse is coupled into the switched cavity with about 90% efficiency. To see this, we can compare the integral of the incident pulse with the peak intensity in the switched case multiplied by τ_{cav}.

In Fig. 7(b) we show the power spectrum of the stored light using the etalon. Four cases are compared: the power spectrum of the pulsed light before it enters the cavity, the spectrum after the switched cavity, and two spectra for a cavity with fixed effective input reflectivity: $R=95\%$ ($V=0.3$ kV) and 68% ($V=1.5$ kV), respectively. The three spectra measured after the light has passed the cavity are taken in identical way using the light leaking through mirror M_4. Their amplitudes can be directly compared. The spectrum of the pulse before it enters the cavity is measured directly and is consequently much stronger. It has been scaled in Fig. 7(b) to a size convenient for comparing its spectral width. We see that for large fixed R the bandwidth is small but so is the overall signal. This case corresponds to filtering out all but the resonant frequency components of the pulse. For smaller but still fixed R the signal becomes larger but so does the bandwidth. Only in the switched case we obtain both the maximum bandwidth reduction and the largest signal. When comparing the switched case to that of fixed input coupling it is useful to consider the ratio power/bandwidth as a figure of merit. For fixed voltage this quantity shows a broad maximum in the range 1.5–2 kV. The power spectra such as those shown in Fig. 7(b) indicate an improvement of about a factor of 2 in this figure of merit when comparing the switched case to the optimal fixed input case.

In principle, the figure of merit of the preceding paragraph should carry over to the time domain; in other words the time traces for the switched case are expected to have longer tails. However, the results of Fig. 7(a) in the time domain indicate a rather smaller difference between the switched case and the optimal choice of fixed input. This apparent discrepancy can be understood by realizing that the experimental pulse is not Fourier-transform limited. The duration of the incident pulse is larger than that resulting from the Fourier transform of the spectrum, rendering the time-domain signals more sensitive

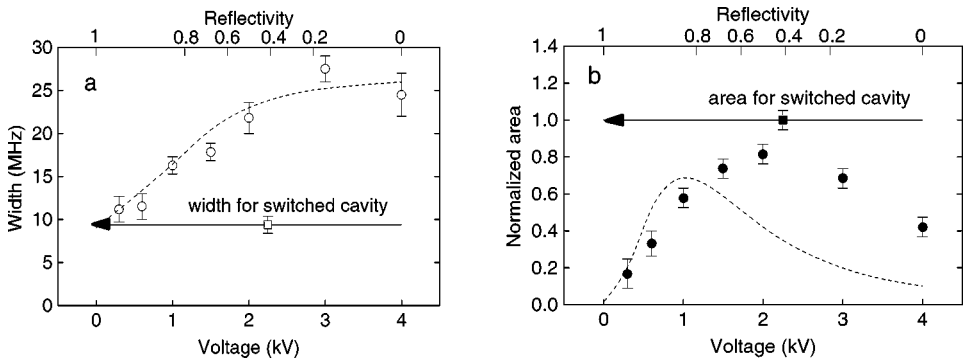

FIG. 8. Summary of experimental results. In (a) we show the width of the power spectrum vs fixed voltage (open circles) and compare it to the switched case (open square). The top axis gives the corresponding effective reflectivity. The dotted line is the theory for the fixed reflectivity case. In (b) we show the area under the spectral peak, normalized to the switched case, which is proportional to the power coupled into the cavity, vs the Pockels cell voltage (filled circles). The filled square corresponds to the switched case. The arrow through this point indicates that the voltage is swept from 4 to 0 kV as the pulse is admitted. The dotted line is a numerical calculation.

to the rather large losses of the cavity. If we make a comparison with the theoretical predictions for the case of 10% loss, for the switched case in Fig. 2(a) and for $R=80\%$ in Fig. 2(b) we find the difference to be approximately as small as in the experiment for roughly comparable parameters.

In Fig. 8 we summarize the results in a more quantitative way. It can be seen that the area under the curve and hence the power coupled into the cavity, in the fixed Pockels cell voltage case, goes through a maximum at about $R=0.5$ ($V=2$ kV) but is always below the power in the switched case. The width on the other hand is always larger than in the switched case, approaching it only for large reflectivity ($V\rightarrow 0$) as expected. The theoretical curve shown in Fig. 8(a) is from Eqs. (6) and (7) with the measured pulse spectrum approximated by a Lorentzian. It contains only two parameters: the spectral width $W=26$ MHz of the incident pulse and the cavity loss rate of 10% (or $R_L=0.9$). Both are determined experimentally in independent measurements. W is measured explicitly and R_L follows from the measured cavity finesse using the reference beam. The data in Fig. 8(a) have been deconvoluted with the instrumental function of the confocal etalon which adds about 1.5 MHz. The good agreement gives confidence in the analysis. The curve of area versus voltage is slightly harder to analyze because it depends more critically on pulse shape and spectral properties. In Fig. 8(b) it is compared with a numerical calculation for a Gaussian pulse with the same parameters as in Figs. 2 and 3. The experimentally observed maximum occurs at a somewhat different value than in the theoretical prediction, but the height of the maximum compared to the switched case is similar. It is likely that the quantitative differences are due to the fact that the experimental pulse is not Gaussian and not transform limited.

VI. CONCLUSION

In this paper we have shown theoretically as well as experimentally that we can do what at first glance seems an impossibility: a pulse is stretched in time thereby reducing its bandwidth, but at the same time its peak intensity increases. This is accomplished using a cavity and varying the efficiency of the input coupler in a way which depends on precise knowledge of arrival time and shape of the pulse. The electric field applied across the Pockels cell acts as a control field and its effect is to adiabatically and reversibly transform the pulse spectrum of finite width into an, in principle, arbitrarily narrow spike.

The present experiment can be seen as a proof of principle of the method. There is considerable room for improvement through careful selection of dedicated quality components resulting in smaller losses. Also the optimization for chirped pulsed is yet to be investigated in detail. We believe the method to be of practical importance in all cases where a narrow bandwidth is needed together with high power. The second-harmonic generation for high-resolution uv spectroscopy is an obvious application. From a practical point of view the experiment as demonstrated here is relatively complex. We believe that in order to realize reliable applications an integrated implementation using fiber optics is desirable as well as practically viable. This would also open the way to a useful application in reversible capture and release experiments.

ACKNOWLEDGMENT

This research was supported by the Dutch Organization for the Fundamental Research of Matter FOM.

[1] F. Brandi, I. Velchev, W. Hogervorst, and W. Ubachs, Phys. Rev. A **64**, 032505 (2001), and references therein.

[2] R. Zinkstok, E.J. Duyn, S. Witte, and W. Hogervorst, J. Phys. B **35**, 2693 (2002).

[3] H. Park, J. Lee, and J. Chang, Phys. Rev. A **53**, 1751 (1996).

[4] S.K. Borisov, M.A. Kuz'mima, and V.A. Mishin, J. Russ. Laser Res. **17**, 332 (1996).

[5] A. Siegman, *Lasers* (University Science Books, New York,

1986).
[6] See e.g., M. Born and E. Wolf, *Principles of Optics* (Pergamon, New York, 1989), Sec. 7.6.
[7] G.D. Boyd and D.A. Kleinman, J. Appl. Phys. **39**, 3597 (1968).
[8] D.F. Phillips, A. Fleischhauer, A. Mair, R.L. Walsworth, and M.D. Lukin, Phys. Rev. Lett. **86**, 783 (2001).
[9] C. Liu, Z. Dutton, C.H. Behroozi, and L.V. Hau, Nature (London) **409**, 490 (2001).
[10] See e.g., G.R. Fowles, *Inroduction to Modern Optics* (Dover, New York, 1968), Sec. 2.5.
[11] T.W. Hänsch and B. Couillaud, Opt. Commun. **35**, 441 (1980).
[12] H.W. Kogelnik, E.P. Ippen, A. Dienes, and C.S. Shank, IEEE J. Quantum Electron. **QE-8**, 373 (1972).